

Remnant living cells that escape cell loss in late-stage tumors exhibit cancer stem cell-like characteristics

Y-L Chen^{1,8}, S-Y Wang^{1,8}, R-S Liu^{1,2,3}, H-E Wang¹, J-C Chen¹, S-H Chiou^{4,5,6}, CA Chang¹, L-T Lin¹, DTW Tan¹ and Y-J Lee^{*,1,7}

A balance between cell proliferation and cell loss is essential for tumor progression. Although up to 90% of cells are lost in late-stage carcinomas, the progression and characteristics of remnant living cells in tumor mass are unclear. Here we used molecular imaging to track the progression of living cells in a syngeneic tumor model, and *ex vivo* investigated the properties of this population at late-stage tumor. The piggyBac transposon system was used to stably introduce the dual reporter genes, including monomeric red fluorescent protein (mRFP) and herpes simplex virus type-1 thymidine kinase (HSV1-tk) genes for fluorescence-based and radionuclide-based imaging of tumor growth in small animals, respectively. Iodine-123-labeled 5-iodo-2'-fluoro-1-beta-D-arabinofuranosyluracil was used as a radiotracer for HSV1-tk gene expression in tumors. The fluorescence- and radionuclide-based imaging using the single-photon emission computed tomography/computed tomography revealed that the number of living cells reached the maximum at 1 week after implantation of 4T1 tumors, and gradually decreased and clustered near the side of the body until 4 weeks accompanied by enlargement of tumor mass. The remnant living cells at late-stage tumor were isolated and investigated *ex vivo*. The results showed that these living cells could form mammospheres and express cancer stem cell (CSC)-related biomarkers, including octamer-binding transcription factor 4, SRY (sex-determining region Y)-box 2, and CD133 genes compared with those cultured *in vitro*. Furthermore, this HSV1-tk-expressing CSC-like population was sensitive to ganciclovir applied for the suicide therapy. Taken together, the current data suggested that cells escaping from cell loss in late-stage tumors exhibit CSC-like characteristics, and HSV1-tk may be considered a theranostic agent for targeting this population *in vivo*.

Cell Death and Disease (2012) 3, e399; doi:10.1038/cddis.2012.136; published online 4 October 2012

Subject Category: Cancer

Tumor growth is dependent on a kinetic model that is based on the progression of cell proliferation and cell loss. The parameters for cell proliferation during tumor progression include the cell-cycle time (T_c), growth fraction (GF), and potential tumor-doubling time (T_{pot}). In contrast, the cell-loss factor is determined by T_{pot} and the actual time for doubling of the tumor volume (T_d).¹ The causes of cell loss include malnutrition and lack of oxygen caused by rapid proliferation, necrosis and apoptosis, immunological attack, escape from the primary site, and exfoliation.² These conditions can be regarded as stresses for cells residing in a rapidly growing tumor. Whether cells escaping from these stresses inherit or obtain resistance abilities is unknown.

The tracking and characterization of living cells in a tumor are important for cancer treatment. Reporter-gene imaging is

an indirect approach to labeling cells for image-based *in vivo* tracking and targeting by different modalities.³ This method is especially important for tracking cell viability *in vivo* because gene transcription and translation occur only in living cells.⁴ In addition, the transmission of genes to progeny is in principle not diminished or diluted if the reporter genes can replicate within the genomes of host cells.⁵ Firefly luciferase and fluorescent proteins are canonical reporter genes used for bioluminescent imaging and optical imaging, respectively. For radionuclide-based reporter-gene imaging, herpes simplex virus type-1 thymidine kinase (HSV1-tk) is commonly used because it can uptake a broad range of radiolabeled nucleoside analogues by substrate phosphorylation for imaging the target cells *in vivo*.⁶ Expression of the HSV1-tk reporter gene can be used for living cell tracking by positron emission

¹Department of Biomedical Imaging and Radiological Sciences, National Yang-Ming University, Taipei, Taiwan, ROC; ²Department of Nuclear Medicine, National PET/Cyclotron Center, Taipei Veterans General Hospital, Taipei, Taiwan, ROC; ³Molecular and Genetic Imaging Core, National Yang-Ming University Medical School, Taipei, Taiwan, ROC; ⁴Department of Medical Research and Education, Taipei Veterans General Hospital, Taipei, Taiwan, ROC; ⁵Institute of Pharmacology, National Yang-Ming University, Taipei, Taiwan, ROC; ⁶Institute of Clinical Medicine, School of Medicine, National Yang-Ming University, Taipei, Taiwan, ROC and ⁷Biophotonics and Molecular Imaging Research Center (BMIRC), National Yang-Ming University, Taipei, Taiwan, ROC

*Corresponding author: Y-J Lee, Department of Biomedical Imaging and Radiological Sciences, National Yang-Ming University, No. 155, Sec. 2, Linong St. Beitou District, Taipei 112, Taiwan, ROC. Tel: +886 2 28267189; Fax: +886 2 28201095. E-mail: yjlee2@ym.edu.tw

⁸These authors contributed equally to this work.

Keywords: cell-loss factor; remnant living cells; cancer stem cells; syngeneic tumor model; piggyBac transposon system; reporter-gene imaging

Abbreviations: CT, computed tomography; FBS, fetal bovine serum; mRFP, monomeric red fluorescent protein; HSV1-tk, herpes simplex virus type-1 thymidine kinase; ¹²³I-FIAU, iodine-123-labeled 5-iodo-2'-fluoro-1-beta-D-arabinofuranosyluracil; SPECT, single-photon emission computed tomography; PET, positron emission tomography; CSC, cancer stem cell; Oct4, octamer-binding transcription factor 4; Sox2, SRY (sex-determining region Y)-box 2; GCV, ganciclovir; GF, growth fraction; ROI, region of interest; FISH, fluorescence *in situ* hybridization; qPCR, semiquantitative real-time PCR; FACS, fluorescence-activated cell sorting; MTT, 3-(4,5-dimethylthiazol-2-yl)-2,5-diphenylterazoliumbromide; 3-D, three-dimensional

Received 19.7.12; revised 24.8.12; accepted 27.8.12; Edited by A Stephanou

tomography (PET) or single-photon emission computed tomography (SPECT), depending on the types of radionuclide-labeled substrates. For instance, iodine-123-labeled 5-iodo-2'-fluoro-1-beta-D-arabinofuranosyluracil (^{123}I -FIAU) is the most reliable radiolabeled nucleoside analogues for SPECT imaging of HSV1-tk gene expression because it exhibits high tumor/background ratio *in vivo*.^{7,8} As described above, the sensitivity and specificity of ^{123}I -FIAU on cancer detection is based on the expression of HSV1-tk reporter gene in the transduced cancer cells. These cancer cells can be distinguished from the non-cancer cells without HSV1-tk genes using the radionuclide imaging modality. Technically, cultured cancer cells are stably transduced with HSV1-tk genes and implanted into animals for tumor formation. Using SPECT imaging, this cancer population can be distinguished from non-cancer portion *in vivo* by injecting ^{123}I -FIAU as a radiotracer that are only accumulated in HSV1-tk gene expressing cancer cells.⁷ Multimodality reporter-gene imaging using coexpressed luciferase/fluorescent proteins and HSV1-tk has been reported to be a powerful tool for basic biological and preclinical research.^{9,10} In addition, PET and SPECT can be merged with computed tomography (CT) to obtain functional/anatomic imaging with high sensitivity and spatial resolution.

Although reporter-gene imaging is widely used for functional studies *in vivo*, concerns regarding the safety and transduction pathways of exogenous genes hamper the clinical application of this approach. Viral-mediated methods are commonly used for the transduction of reporter genes, but the uncontrolled infection and random genomic integration of genes of interest currently limit the clinical application of these methods.¹¹ In contrast, nonviral gene delivery is more acceptable in the clinic because biocompatible materials can be used, and the safety of these approaches is relatively easily assessed by pharmacokinetic and pharmacodynamic studies.¹² The piggyBac transposon system has recently attracted a great deal of attention because the system is a nonviral gene-delivery approach that uses DNA-transposition ability for the stable expression of exogenous genes via a 'cut-and-paste' mechanism.¹³ The beauty of this system includes its known integration sites at 'TTAA' sequences and intron-preferred positions, mammalian compatibility, large cargo capacity, and its ability to be removed from the integration site without changing the DNA sequence.¹⁴ In practice, this system requires a helper plasmid that encodes the piggyBac transposase gene to facilitate the transposition of exogenous gene.¹⁵ The piggyBac transposon system has been applied in induced pluripotent stem cells, cancer research, and immunotherapy.^{16,17} However, the use of this system has been less frequently reported in multimodality reporter-gene imaging of tumor progression.

Cancer stem cells (CSCs, or tumor-initiating cells) belong to the hierarchy model that a subset of rare cell population inherits stem cell-like characteristics, including self-renewal and generation of non-tumorigenic progeny.¹⁸ This theory has intrigued many researchers in recent years because CSCs are resistant to chemoradiotherapy and are likely to be the cause of tumor recurrence and metastasis.¹⁹ However, the identification of CSCs *in vivo* remains a challenge because of the lack of suitable markers for this purpose. If CSCs naturally

resist environmental stresses, it would be speculated that this population may also escape from cell loss during tumor progression. More evidence is required to support this hypothesis.

The percentage of cell loss during tumor progression is approximately 40–90%, depending on the cancer type.¹ The remnant viable cells may be important for promoting tumor growth and metastasis. Reporter-gene imaging should be ideal to track these living cells for further investigation of their characteristics. In this study, we established a syngeneic tumor model derived from 4T1 murine breast carcinomas transduced with monomeric red fluorescent protein (mRFP)/HSV1-tk dual reporter genes using the piggyBac transposon system. A combination of optical imaging and SPECT/CT fusion imaging using ^{123}I -FIAU as a probe was exploited to track the remnant living cells in late-stage primary tumors. Furthermore, *ex vivo* studies showed that the surviving cells exhibited CSC-like characteristics. These findings may contribute to therapeutic designs for cancer treatment.

Results

Establishment of the transgenic tumor cells with imaginable dual reporter genes using the piggyBac transposon system.

In this study, the piggyBac transposon system was used to establish stable cancer cell lines harboring mRFP and HSV1-tk reporter genes that were driven by different promoters (Supplementary Figure 1A). The Act4-PBase helper plasmid and PB-2 R-puro donor plasmid were cotransfected in human 293 T cells, H1299 cells, MDA-MB-231 cells, and mouse 4T1 cells. The expression of reporter genes was sustained in each cell type for longer than 2 weeks, but cells transfected with donor plasmid only lost reporter-gene expression in 4 days (Supplementary Figures 1B and C). To enrich pure stable cells for *in vivo* imaging, we sorted the piggyBac-transfected cells expressing mRFP by fluorescence-activated cell sorting (FACS). Here we focused on 4T1 cells because a syngeneic tumor model was subsequently established. Two days after transfection, 0.7–0.9% of mRFP-expressing 4T1 cells could be sorted (Supplementary Figure 2). The expression of reporter genes was sustained in 4T1 cells cotransfected with both plasmids (named 4T1-PB-2R/PBase cells) for up to 60 days without puromycin selection, but it was diminished in 4T1 cells transfected with PB-2 R-puro only (named 4T1-PB-2 R cells) after 7 days of culture (Figure 1a). The transposition assay was also used to confirm the requirement for the Act-PBase helper plasmid in the stabilization of reporter genes in 4T1 cells by puromycin selection (Supplementary Figure 3). The sustained expression of HSV1-tk in 4T1-PB-2R/PBase cells was determined using the western blot assay (Figure 1b). HSV1-tk remained functional as determined by a cell-uptake assay using ^3H -FIAU (Figure 1c). Furthermore, 4T1-PB-2R/PBase cells, but not 4T1-PB-2R cells, were sensitive to ganciclovir (GCV), which is a prodrug phosphorylated and activated by HSV1-tk to cause cell death (Supplementary Figure 4). Moreover, the fluorescence *in situ* hybridization (FISH) assays showed that the long-term expression of reporter genes was associated with the chromosomal integration of reporter genes in the

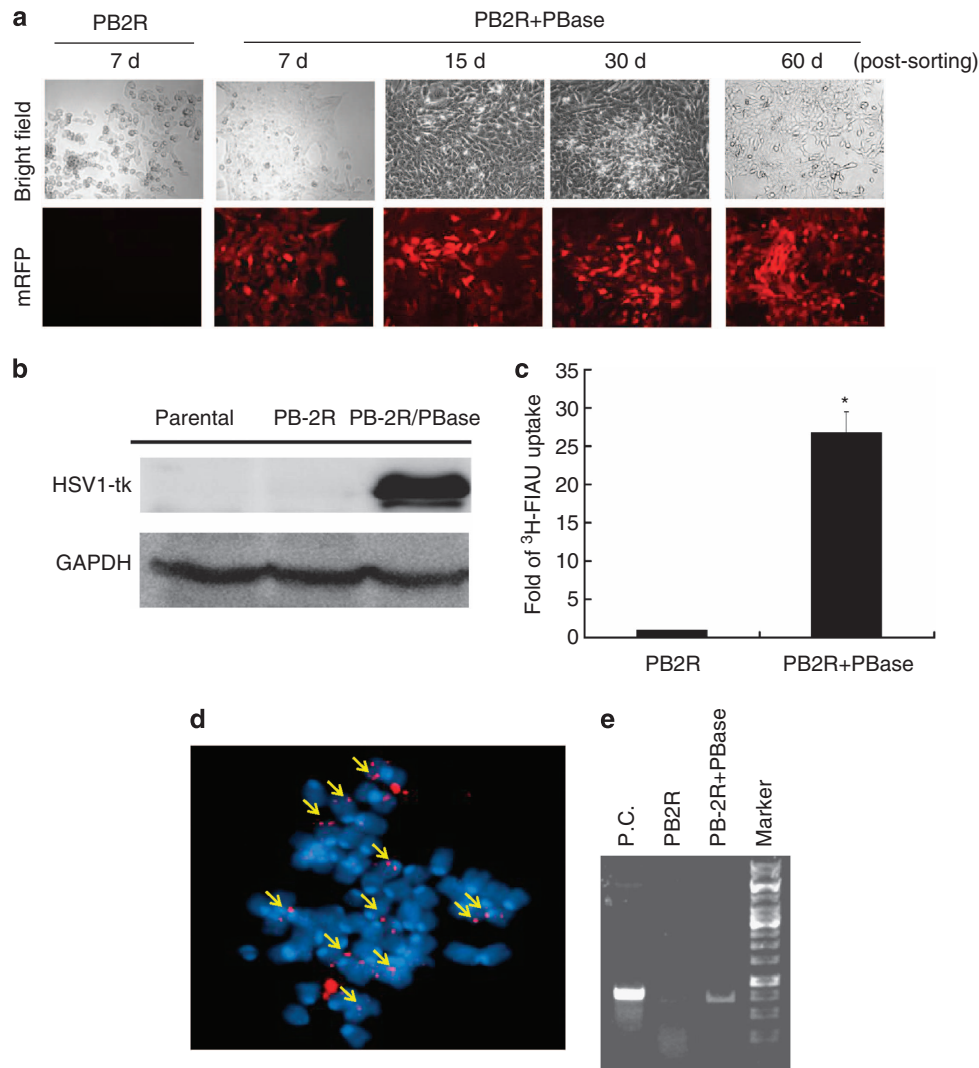


Figure 1 *In vitro* functional analysis of reporter genes transduced into 4T1 cells using the piggyBac transposon system. (a) Tracking of mRFP expression in sorted 4T1-PB-2R/PBBase and 4T1-PB-2R cells in a time-course manner. (b) Western blot analysis of HSV1-tk expression in mRFP-sorted cells cultured for 60 days. (c) Cell-uptake assay to detect HSV1-tk activity in cells treated with ³H-FIAU. The data represent the means of three independent experiments \pm S.D. * $P < 0.05$. (d) FISH assay for visualizing the integration of the mRFP reporter gene in the chromosomes of 4T1-PB-2R/PBBase cells (the mean copy number was approximately 14 by counting six cells). (e) Genomic PCR for amplifying the mRFP DNA sequence from cellular chromosomes. P.C., a positive control by amplifying the mRFP gene from the original PB-2R-puro plasmid. The PCR product was 0.67 kb

genomes of 4T1-PB-2R/PBBase cells (Figure 1d). This observation was also demonstrated using the genomic PCR (Figure 1e). This 4T1-PB-2R/PBBase cancer cell lines were subsequently used for fluorescence- and radionuclide-based imaging *in vivo*.

Imaging of tumor formation in the syngeneic tumor model. To establish the syngeneic tumor model, 4T1-PB-2R/PBBase and 4T1-PB-2R tumor cells were subcutaneously implanted into BALB/c mice followed by imaging the mRFP expression. The growth rates of tumors formed by these two transduced cell types and the untransduced parental 4T1 cells were similar, indicating that genomic integration of reporter genes did not affect cell proliferation (Figure 2a). Although both transduced cell types formed tumors *in vivo*

within 7 days, the fluorescent signal was only detected in tumors formed by 4T1-PB-2R/PBBase cells, but not by 4T1-PB-2R cells, within a cell number-dependent manner (Figure 2b). The results of tumorous images formed by 4T1-PB-2R/PBBase cells were quantified and compared among different cell amount after 1 day and 7 days of subcutaneous (s.c.) implantation (Figure 2c). Furthermore, the histological investigation was used to demonstrate the coexpression of mRFP and HSV1-tk genes in this syngeneic tumor model (Supplementary Figure 5).

Detection of the remnant living cells in tumor progression using the dual reporter-gene imaging. Rapid tumor growth is accompanied by an increase of cell loss at the primary site. However, the characteristics of the remnant

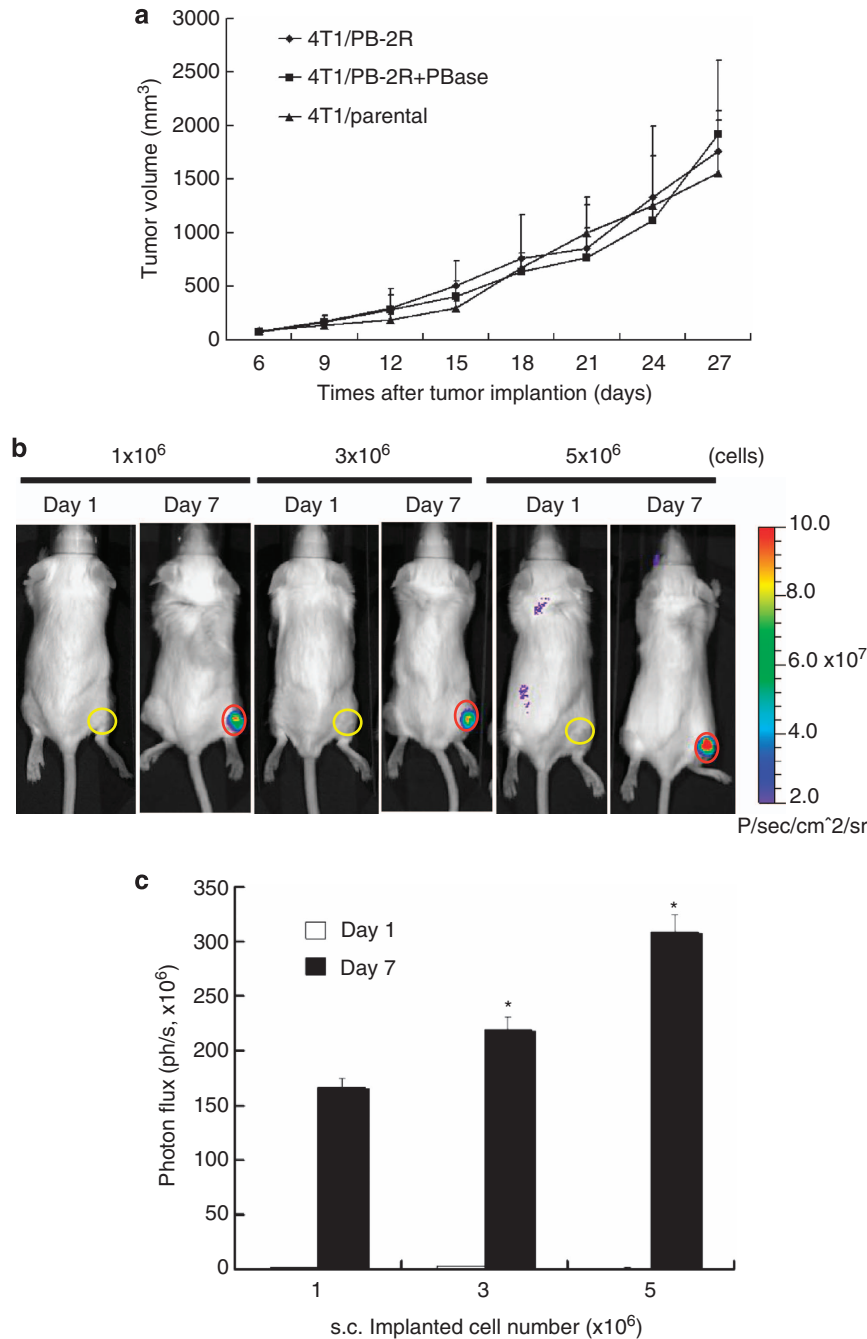


Figure 2 Imaging of tumor growth in the syngeneic tumor model. (a) The growth rates of tumors formed by parental 4T1 cells, 4T1-PB-2R/PBBase cells, and 4T1-PB-2 R cells were measured and compared using calipers ($n = 6$). (b) Use of the IVIS 50 system for imaging the level of the mRFP signals in tumors 1 day and 7 days after initial seeding. The ROIs are indicated by circles. (c) Quantification of the ROI in (b). * $P < 0.05$ compared with 1×10^6 cells at day 7

living cells in the tumor mass are less investigated. Hence, we determined to track the living 4T1-PB-2R/PBBase cells during tumor progression *in vivo* based on the reporter-gene imaging. Figure 3a represented the agendas for imaging the expression of mRFP and HSV1-tk after s.c. implantation of 4T1-PB-2R/PBBase breast carcinomas (Figure 3a). For the fluorescence imaging, the mRFP signal at the tumor site was increased in the first 2 weeks, but was decreased thereafter ($n = 12$) (Figure 3b). These results suggest that the amount

of viable cells in the primary tumor is reduced during tumor progression.

To better understand the spatial and temporal characteristics of viable 4T1-PB-2R/PBBase cells in implanted tumors, mice were i.v. injected with ¹²³I-FIAU to track cells expressing HSV1-tk gene using the microSPECT/CT. The results showed that the accumulation of ¹²³I-FIAU in the primary tumor site was detected on 7 days after implantation, but the ratio of accumulation tended to reduce during tumor

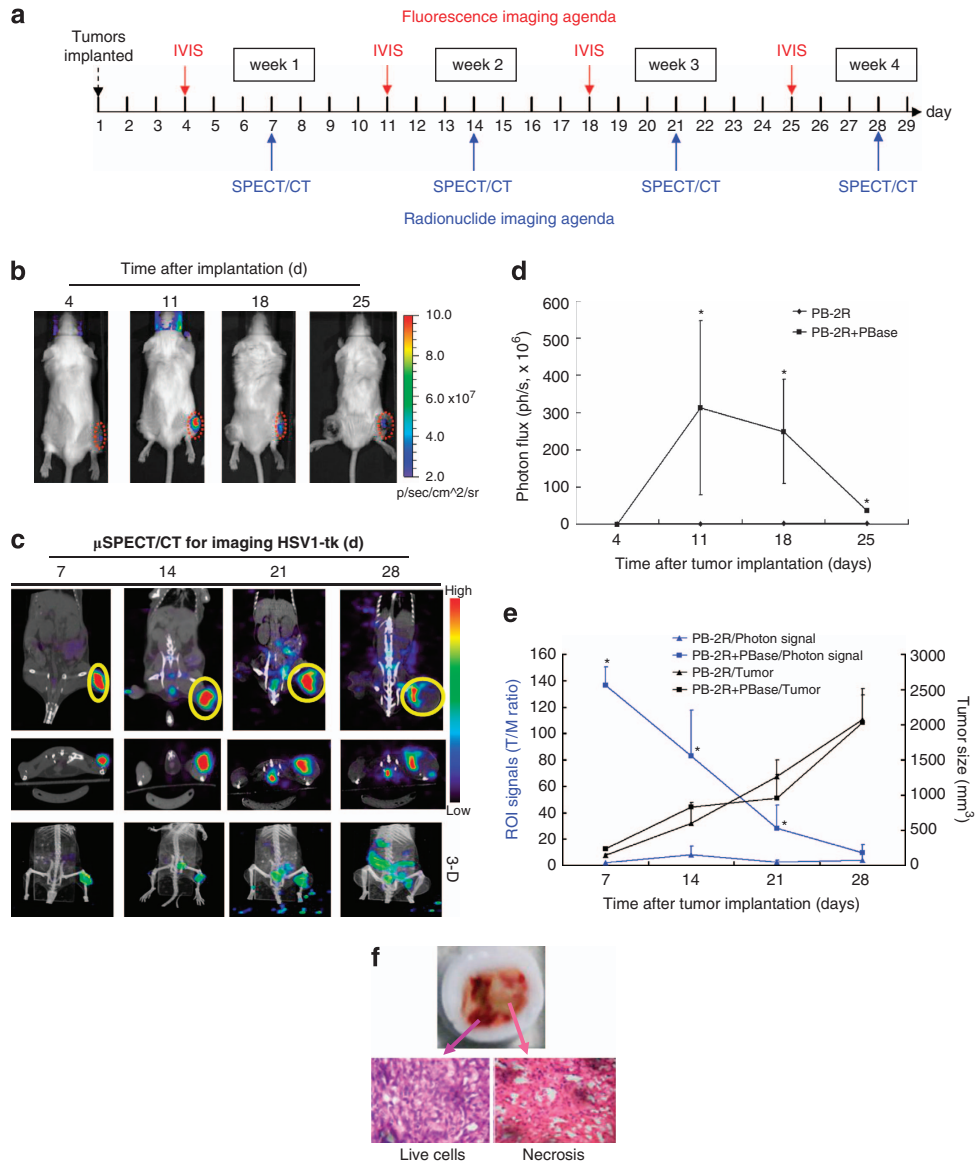


Figure 3 Time-course-dependent tracking of living cells in syngeneic tumors by multimodality reporter-gene imaging. **(a)** The agendas of fluorescence imaging and radionuclide imaging of tumor progression using IVIS 50 system and microSPECT/CT, respectively. **(b)** The fluorescence imaging of tumor progression after s.c. injection of 4T1-PB-2R/PBBase and 4T1-PB-2 R cells into BALB/c mice. **(c)** MicroSPECT/CT imaging of HSV1-tk expression in formed tumors. The reconstructed 3-D images of tumors at different time point were also involved. **(d)** Quantification of photon signal determined by ROIs of the fluorescence imaging. **(e)** Quantification of ROIs (blue lines) from radionuclide tomographic images and the relationship to the tumor size (black lines) at different time point of tumor imaging. Mean counts of photon signals were quantified. Each datum represents a mean of independent values \pm S.D. * $P < 0.05$ ($n = 12$). **(f)** Frozen sections were stained with H&E to distinguish the live tissues (left panel) and necrotic region (right panel) in the primary tumor

progression (Figure 3c). This observation was further confirmed by the reconstructed three-dimensional (3-D) imaging of living cells in the tumor mass (Figure 3c and Supplementary Video 6). The fluorescence and radionuclide imaging of tumors were subsequently quantified by the selected region of interest (ROI) of each image. The amount of photon flux of fluorescence imaging was reduced after 11 days of tumor growth (Figure 3d). The ROI signal of radionuclide imaging was also decreased after 7 days of tumor implantation, even though the tumor size was increased (Figure 3e). The imaging results of the fluorescent and radionuclide images were also

attempted to merge to display the quantificational correlations of living cell signal at the primary tumor (Supplementary Figure 7). Moreover, the histopathological investigation were applied to confirm that functional tumor cells only occupied part of the late-stage tumor (Figure 3f). Apparent necrotic region was also detected. Additionally, the anatomic examination of visceral showed that at least liver contained suspected tumor cells (Supplementary Figure 8A). They were subsequently confirmed by visualizing the expression of mRFP as shown in the primary tumor formed by 4T1-PB-2R/PBBase cells (Supplementary Figure 8B).

Remnant living tumor cells exhibit CSC-like characteristics through *ex vivo* examination. Cell lost from rapidly growing tumors is caused by intrinsic and extrinsic stresses. It is speculated that cells escaping from these stresses may perform particular abilities to survive and promote the tumor progression. Here we investigated whether the remnant living cells in the late-stage tumors exhibited the characteristics of CSCs, which are supposed to be resistant to environmental stresses for tumor viability. Based on the results of the multimodality reporter-gene imaging described above, the *ex vivo* experiments were performed to isolate the remnant living 4T1-PB-2R/PBase cells from late-stage tumors formed in separate mice. First, the sphere-formation assay showed that mRFP-expressing mammospheres were formed in *in vivo* tumor-isolated 4T1-PB-2R/PBase cells, but not in parental and original transduced 4T1 cells after seeding (Figure 4a). The number of mammospheres from *ex vivo* 4T1-PB-2R/PBase cells was greater than that of parental 4T1 cells after 4 days of initial seeding (Figure 4b). These observations suggest that remnant living cells in late-stage tumors exhibit increased sphere-forming capacity, which is one of the CSC characteristics.

Two general CSC biomarkers, octamer-binding transcription factor 4 (Oct4) and SRY (sex-determining region Y)-box 2 (Sox2), were subsequently examined using semiquantitative

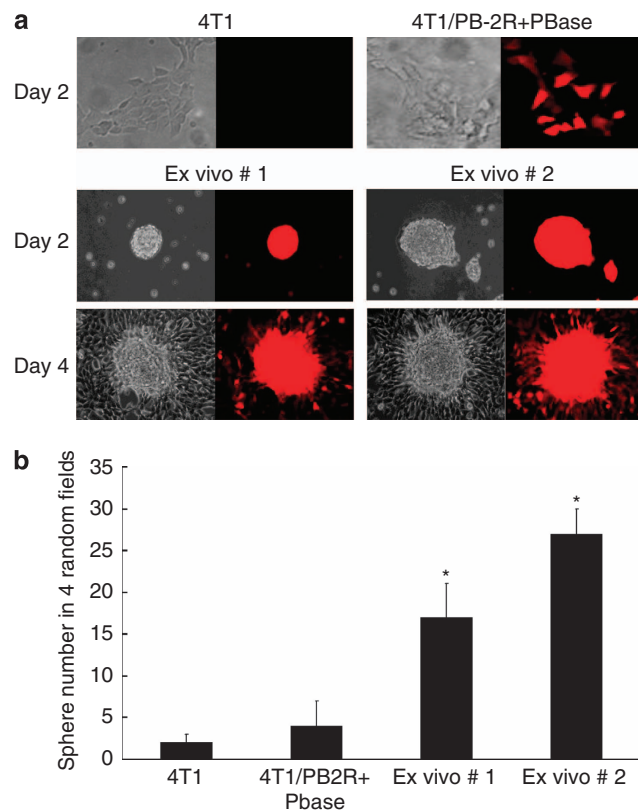


Figure 4 Increase of sphere formation by the remnant living cells isolated from the late-stage primary tumors. (a) Comparison of sphere formation in parental 4T1 cells, original transduced 4T1-PB-2R/PBase cells, and two *ex vivo* isolated remnant living cells from the late-stage tumors. (b) Quantification of spheres. The sphere numbers were obtained from four random fields examined under the microscope. * $P < 0.05$

real-time PCR (qPCR). Compared with parental 4T1 cells, *ex vivo* 4T1-PB-2R/PBase cells exhibited upregulation of Oct4 and Sox2 mRNA (Figures 5a and b). The transcriptional activity of Oct4 was also increased in *ex vivo* 4T1-PB-2R/PBase cells in an Oct4 promoter assay (Figure 5c). Furthermore, the protein levels of Oct4, Sox2 and another CSC-associated biomarkers CD133 were upregulated in *ex vivo* 4T1-PB-2R/PBase cells isolated from late-stage tumors formed in different mice (Figure 5d). No significant change of these biomarkers in original 4T1-PB-2R/PBase cells with routine subculture before *in vivo* implantation. Taken together, the remnant living cells escaping from cell loss in late-stage tumors display CSC-like characteristics, at least in part.

HSV1-tk-expressing remnant living tumor cells with CSC-like characteristics are sensitive to GCV. The expression of HSV1-tk was also preserved in remnant 4T1-PB-2R/PBase living cells isolated from the late-stage tumor (Figure 6a). HSV1-tk is the first identified suicide gene that is considered safe for gene therapy in transduced cancer cells after exposed to GCV.²⁰ Given the remnant 4T1-PB-2R/PBase living cells isolated from the late-stage tumor *in vivo* exhibited CSC-like characteristics, we examined whether they remained sensitive to GCV. We first examined the sphere-formation capacity and side population percentage of original 4T1-PB-2R/PBase cells before and after GCV to determine whether CSCs would be enriched by this treatment. The results showed that both CSC-related characteristics were not increased in GCV-treated 4T1-PB-2R/PBase cells, suggesting that this method would not increase CSC population *in vitro* (Supplementary Figure 9). Subsequently, the 3-(4,5-dimethylthiazol-2-yl)-2,5-diphenylterazoliumbromide (MTT) assay showed that the cell viability was greatly reduced in the isolated remnant 4T1-PB-2R/PBase living cells with CSC-like properties after they were exposed to different concentrations of GCV (Figure 6b). Thus, HSV1-tk is not only important for reporter-gene imaging of CSC-like living cells in tumors but also a potent therapeutic agent in this cell population.

Discussion

The current data demonstrate that tumor cells escaping from cell loss and surviving in the late-stage tumors contain CSC-like characteristics. Conventionally, CSCs are believed to emerge after the chemo- and radiotherapy because of the generation of resistance. Nevertheless, we found that cells would spontaneously express CSC-like characteristics when they were not lost in the late-stage tumor. The reporter-gene imaging based on the optical and microSPECT/CT modalities is essential for tracking the spatial and temporal characteristics of these remnant living cells *in vivo*. It would be of interest to further investigate if the stress of cell-loss factor can promote the generation of CSC-like population during tumor progression *in vivo*.

CSCs have been reported to be a rare population that is related to the recurrence and metastasis of advanced tumors.²¹ For experimental purposes, putative CSCs can be isolated from cultured cell lines using sphere formation and FACS based on Hoechst 33342 dye exclusion or

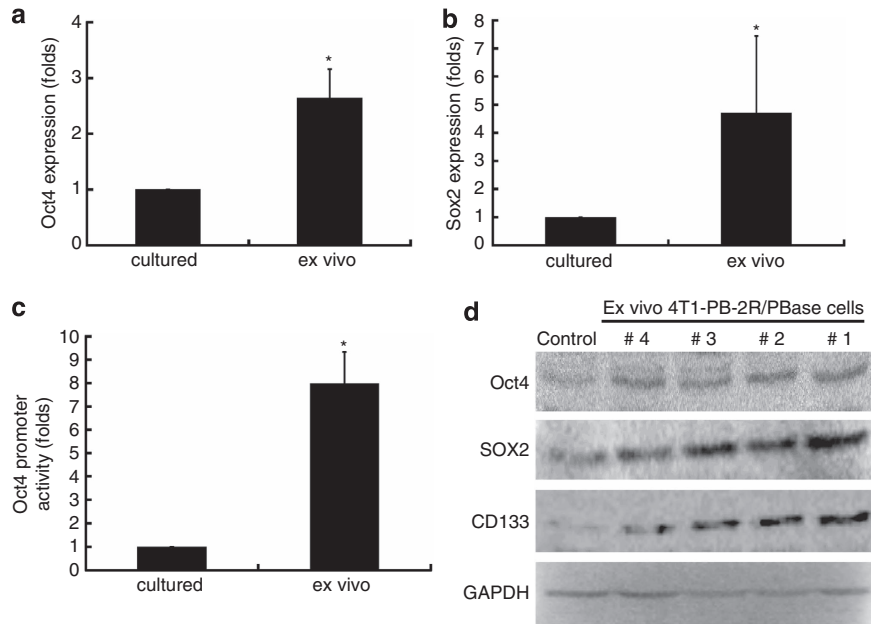


Figure 5 Expression of CSC-related markers in *ex vivo* isolated remnant living cells. (a) Oct4 mRNA and (b) Sox2 mRNA expression was compared between cultured and *ex vivo* isolated remnant living 4T1-PB-2R/PBBase cells using qPCR. (c) Luciferase reporter-gene assay for investigating the Oct4 transcriptional activity in parental cells and isolated remnant living cells. The data represent the means of four independent experiments \pm S.D. * $P < 0.05$. (d) Western blot analysis to compare the expression of Oct4, Sox2, and CD133 proteins between cultured cells and four *ex vivo* isolated remnant living cells

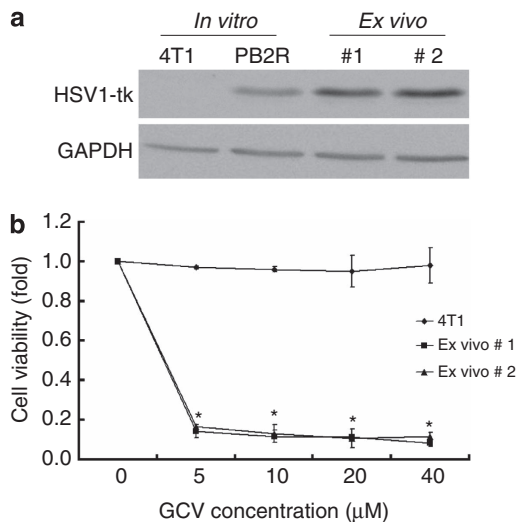


Figure 6 Remnant living cells expressing HSV1-tk are sensitive to GCV. (a) Western blot analysis compared the expression of the HSV1-tk reporter gene in *ex vivo* 4T1-PB-2R/PBBase cells and the original transduced 4T1-PB-2R/PBBase cells. (b) MTT assay compared the viability between HSV1-tk-expressing CSC-like cells and parental 4T1 cells after GCV treatment. Each datum represents the mean of five independent experiments \pm S.D. * $P < 0.05$

fluorescein-conjugated antibodies against the expression of stem cell markers.²² However, several lines of evidence have argued that cells selected using these *in vitro* methods exhibit negative or even opposite tumorigenic properties from those predicted by the CSC hypothesis.^{23–25} In addition, the currently available markers for *in vitro* CSC selection are not very suitable for *in vivo* application.²⁶ The lack of *in vivo*

evidence of CSCs would impede the clinical application of this theory. Based on our *ex vivo* experimental results, cells survived in late-stage tumor would exhibit CSC-like characteristics. Therefore, it suggests that remnant living cells in advanced tumor are the CSCs *per se*. The reporter-gene imaging is likely the most appropriate approach to tracking these living tumor cells *in vivo*, at least in the preclinical study.

The reporter-gene imaging is based on the principle of molecular biology to track living cells *in vivo*. This approach is also appropriate for *in vivo* imaging of CSCs.²⁷ For instance, Vlashi *et al.*²⁶ have established a short half-life version of the fluorescent ZsGreen reporter gene and demonstrated that CSCs contain reduced 26S proteasomal activity. They showed that a local fractionated irradiation of tumor *in vivo* steadily increased the ZsGreen-positive cells with CSC characteristics. In our study, we used constitutively expressed mRFP and HSV1-tk reporter genes to track the remnant living cells in advanced tumor. Interestingly, after transfection of a short half-life version of green fluorescent protein (d2GFP) into these remnant living cells, they also expressed sustained fluorescent signals compared with parental cells using the fluorescence microscopy (data not shown). Therefore, use of reporter-gene imaging to track the remnant living cells in advanced tumor is likely a direct approach to find CSCs *in vivo*.

The fluorescence imaging has been claimed to be ideal for *in vivo* detection of the rare cell population in tumors.²⁸ Additionally, the radionuclide-based imaging is essential for tracking functional cells in deep tissues using the 3-D reconstruction. Indeed, mutant HSV1-tk has been combined with firefly luciferase for imaging the differentiation of mesenchymal stem cells using PET and bioluminescence dual imaging modalities.⁹ Here we provide a proof-of-concept

that a similar dual reporter-gene imaging using mRFP and HSV1-tk can also track CSC-like viable cells in late-stage tumors using the syngeneic tumor model. These two reporter genes are driven by separate promoters. This is important for tracking functional cells *in vivo* using the multimodality imaging because reduction of both imaging signals in tumors should be due to cell loss but not inactivation of one of the reporter genes. The current findings would encourage us to apply this approach to track the remnant living cells with CSC-like characteristics using the xenograft tumor model in the future.

The syngeneic tumor model is ideal for exploring the tumor growth and metastasis in the context of a normal immune system. This model is also especially particularly important for the study of the growth niche for CSC progression.²⁹ Bioluminescent reporter-gene imaging based on luciferase expression has been reported to track the growth and metastasis of the 4T1 tumor model of late-stage breast cancer.³⁰ Our 4T1-PB-2R/PBase tumor model contains a HSV1-tk reporter gene that can obtain better spatial resolution with 3-D images for detecting tumor growth and potent metastasis using the microSPECT/CT. According to the *ex vivo* investigation of mRFP expression, we were able to identify the 4T1-PB-2R/PBase cells that existed not only in the primary site but also in the liver in late-stage tumor using the fluorescence microscope. Therefore, a multimodality-based reporter-gene system should be essential for investigating the behaviors of living tumor cells in a syngeneic tumor model *in vivo* and *ex vivo*.

The theory of tumor kinetics was proposed approximately half a century ago.^{1,31} The cell-loss factor accounts for the fact that the measurable tumor growth rate is much slower than the prediction from the cell-cycle time of each individual cell and GF. In general, the cell-loss factor tends to be larger (up to 90%) in carcinomas that usually exhibit apoptosis during progression.² The remnant living cells in this tumor type are essential for determining the efficacy of chemotherapy and radiotherapy because tumors with a high level of cell-loss factor respond quickly to these treatments. Characterization of these living cells should be important for the design of therapeutic strategies. Because the current data suggest that these remnant living cells contain CSC-like characteristics, it would be possible to precisely track these population using CSC-specific probe to identify their position and quantity in the future.

CSCs have been reported to be a rare population that is related to the recurrence and metastasis of advanced tumors.²¹ For experimental purposes, putative CSCs can be isolated from cultured cell lines using sphere formation and FACS based on Hoechst 33342 dye exclusion or fluorescein-conjugated antibodies against the expression of stem cell markers.²² However, several lines of evidence have argued that cells selected using these *in vitro* methods exhibit negative or even opposite tumorigenic properties from those predicted by the CSC hypothesis.^{23–25} In addition, the currently available markers for *in vitro* CSC selection are not very suitable for *in vivo* application.²⁶ The lack of *in vivo* evidence of CSCs would impede the clinical application of this theory. Based on our *ex vivo* experimental results, cells survived in late-stage tumor would exhibit CSC-like

characteristics. Therefore, it suggests that remnant living cells in advanced tumor are the CSCs *per se*. The reporter-gene imaging is likely the most appropriate approach to track these living tumor cells *in vivo*, at least in the preclinical study.

Although CSCs have been regarded as potent targets for cancer therapy, these cells usually exhibit resistance to chemotherapy and radiotherapy. As a reporter gene, we showed that the HSV1-tk expressed in the CSC-like population from 4T1 cells was susceptible to GCV, suggesting that HSV1-tk-based suicide gene therapy may be effective in CSCs. These results are consistent with a previous report showing that lentiviral vector-mediated HSV1-tk gene therapy can cause remission of cancer stem-like glioblastoma xenografts.³² Therefore, further investigation of whether the HSV1-tk gene can be used as a theranostic agent for targeting CSCs would be of interest.

In summary, we utilized reporter-gene imaging for *in vivo* detection of living cells during tumor progression using the 4T1 syngeneic tumor model. For late-stage tumors, the remnant living cells exhibit CSC-like characteristics, which may explain, at least in part, the tumor metastasis and chemoradiotherapeutic resistance that may cause the recurrence. Because clinically detected human cancers have usually reached mid to late stages, the hypothesis that remnant living cells contain CSC-like characteristics will provide important information for the design of novel therapeutic strategies for cancer treatment.

Materials and Methods

Cell lines, plasmid and stable transfection. Human embryonic kidney 293T cells (provided by National RNAi Core Facility, Academia Sinica, Taipei, Taiwan, originated from American Type Culture Collection (ATCC no. CRL-11268)), human non-small lung cancer H1299 cells,³³ and human breast cancer MDA-MB-231 cells (a kind gift from Dr. Jeng-Jong Hwang at National Yang-Ming University, originated from ATCC no. HTB-26) were cultured in Dulbecco's modified Eagle's medium supplemented with 10% fetal bovine serum (FBS), 2 mM L-glutamate, 50 U/ml penicillin and 50 µg/ml streptomycin (Invitrogen Inc., Carlsbad, CA, USA). The cell lines were maintained at 37 °C in a humidified incubator containing 5% CO₂ and were routinely passaged every 2 days. 4T1 murine breast carcinomas (a kind gift from Dr. Yueh-Hsing Ou at National Yang-Ming University, originated from ATCC no. CRL-2539), 4T1-PB-2R cells, and 4T1-PB-2R/PBase cells were cultured in RPMI1640 medium supplemented with 10% (v/v) FBS, 100 U/ml of penicillin, and 100 mg/ml streptomycin. 4T1 breast carcinomas were isolated from the mammary tumor of BALB/c mouse according to the product description of ATCC.

The PiggyBac transposon system including the PB-tk-mRFP reporter plasmids and Act-PBase helper plasmid were kindly provided by Dr. Congjian Xu (Fudan University, People's Republic of China).³⁴ PB-tk-mRFP was further modified by inserting a puromycin-resistance cassette into the *Bgl*II and *Bam*HI sites to obtain a new construct named PB-2R-puro. For cotransfection, PB-2R-puro was mixed with Act-PBase at the optimal ratio and transfected into cells using jetPEI transfection reagent (Polyplus-Transfection Inc., New York, NY, USA). Transfected cells were sorted using a BD FACSCalibur system (BD, Franklin Lakes, NJ, USA) equipped with an air-cooled argon laser excited at 488 nm. The cells were expanded and maintained in normal medium for further experiments.

Western blot analysis. The procedure of western blot analysis was performed as described previously.³³ Anti-HSV1-tk (Santa Cruz Biotechnology Inc., Santa Cruz, CA, USA), anti-Oct4, anti-Sox2 (Abcam, Cambridge, MA, USA), and anti-CD133 (Cell Signaling Technology, Danvers, MA, USA) antibodies were used according to the conducted experiments.

Measurement of HSV1-tk activity *in vitro*. The activity of HSV1-tk was determined by a cell-uptake assay and MTT assay. For the cell-uptake assay,

1×10^5 cells were seeded in 24-well culture plates and cultured overnight. ^3H -FIAU ($1 \mu\text{Ci}$ per well) was then added to each well for 2 h. The radioactivities in the cells and in the supernatant were determined separately and normalized using a gamma counter (Wallac 1470 Wizard; Perkin Elmer, Waltham, MA, USA). For the MTT assay, 800 cells were seeded in 96-well plates and cultured overnight. Different concentrations of GCV (Sigma-Aldrich, Inc., St. Louis, MO, USA) were added to the wells and maintained for 4 days. MTT (1 mg/ml) (Sigma-Aldrich, Inc.) was then added to the cells for 4 h, dissolved in dimethyl sulfoxide, and measured at an absorbance of 570 nm on an ELISA plate reader (Bio-Tek Instruments, Winooski, VT, USA).

Fluorescence *in situ* hybridization. The FISH analysis was performed according to previous reports.³⁵ The PB-2R-puro plasmid was labeled with biotin-16-dUTP using the nick translation (BioNick kit; Invitrogen Inc.). The fluorescein-conjugated avidin was used to detect biotin-16-dUTP-labeled PB-2R-puro hybridizing to the chromosomes.

Genomic PCR. The genomic DNA was extracted using DNAzol (Invitrogen Inc.). The forward and reverse primers for amplifying the mRFP sequence were 5'-CCATGGGCTGGGAGGCCTCC-3' and 5'-TTAACCCCTAGAAAGATAGTCTG-3', respectively. The PCR protocol was followed by the manufacturer's instruction.

Mice and syngeneic tumor model. The 6-week-old female BALB/c mice were purchased from the Laboratory Animal Center, National Taiwan University College of Medicine (Taipei, Taiwan, ROC). For this study, 18 mice were used for s.c. tumor implantation and imaging processes. The amount of mice used for different experiments has been described in the results. The animal use protocols have been reviewed and approved by the Institutional Animal Care and Use Committee of National Yang-Ming University (approval number: 981225).

Based on the experimental design, 4T1 cells and the derived stable cell lines expressing reporter genes were implanted into each mouse at subcutaneously. The tumor volumes at s.c. positions were measured by caliper every 3 days and calculated using the following formula: Volume = Length (mm) \times Width² (mm²)/2.

Tumor imaging. For the fluorescence imaging, an IVIS 50 system (Xenogen Inc., Alameda, CA, USA) was used to image the expression of mRFP in the tumors formed by 4T1-PB-2 R/PBase and 4T1-PB-2R cells. Mice were anesthetized using 2% isoflurane during the imaging process. The ROIs were acquired based on the signals emitted from the tumor positions and semiquantified as photons per second. Data quantification was analyzed using the IGOR-PRO Living Imaging Software (WaveMetrics, Inc., Lake Oswego, OR, USA).

MicroSPECT/CT tumor imaging was based on a FLEX Triumph preclinical imaging system (Gamma Medica-Ideas, Inc., Northridge, CA, USA) as previously described.³⁶ The Lugol's solution (potassium iodide tablets) were given 1 h prior to i.v. injection of ^{123}I -FIAU (16 mCi/kg). Six hours later, the mice were anesthetized using 2% isoflurane mixed with oxygen and scanned by CT using 512 slides for anatomic coregistration. Subsequently, a static SPECT sequence involving eight frames was conducted. Thirty-two projections (50 s) were acquired over 180° , which formed a 60×60 matrix for a total imaging time of 30 min per frame. The tumor images were viewed, reconstructed for 3-D images, and quantified using a free Amide software (SourceForge, Geeknet Inc., Fairfax, VA, USA).³⁷

Sphere-formation assay. Five-thousand cells were seeded in a 10-cm noncoated plate. The conditional medium contained serum-free DMEM/F12, 10 ng/ml of epithelial growth factor, 10 ng/ml of basic fibroblast growth factor, 10 ng/ml of insulin, and 5 ml of N2 (Gibco Inc., Grand Island, NY, USA). Formed spheres were visualized under a bright-field microscope.

Real-time PCR analysis. Total RNA was extracted using TRIzol reagent (Invitrogen Inc.) and was purified using Direct-zol RNA miniprep kit (Zymo Research Corporation, Irvine, CA, USA) to remove genomic DNA contamination according to the manufacturer's instruction. An amount of $1 \mu\text{g}$ of purified total RNA was subjected to cDNA synthesis using SuperScript II reverse transcriptase (Invitrogen Inc.). For qPCR analysis of Oct4 gene expression, the forward primer was 5'-TTGGGCTAGAGAAGGATGTGGTT-3', and the reverse primer was 5'-GGAAAGGGACTGAGTAGAGTGTGG-3'. For Sox2 gene, the forward primer was 5'-GCACATGAACGGCTGGAGCAACG-3', and the reverse primer was 5'-TGCTGCGAGTAGGACATGCTGTAGG-3'.³⁸ For human/mouse β -actin gene, forward primer was 5'-GGAAATCGTGCATTAAG-3', and the reverse

primer was 5'-GGCCATCTCTTCTGCTCGAAGT-3'. The experiments were conducted using the Master SYBR Green reagent mixed with cDNA templates and corresponding primers, and the reactions were performed in a StepOnePlus machine (Applied Biosystems Inc., Carlsbad, CA, USA). The quantification of mRNA level and the melting curve analysis were completed by the bundled software (StepOne software version. 2.1, Applied Biosystems Inc.).

Oct4 promoter assay. The PGL4.2-Oct4 luciferase reporter-gene construct containing the human Pou5f (Oct4) gene promoter was a gift from Dr. Mu-Hwa Yang at National Yang-Ming University. This construct was transfected into cells for 48 h using jetPEI (Polyplus-Transfection Inc.) according to the manufacturer's instructions. The transfected cells were lysed and subjected to the luciferase assay using 50 mM of D-luciferin. The illuminant intensity was measured using the Wallac Victor 2 Multi-label Counter (Perkin Elmer). Each datum was normalized to the total protein level.

Statistical analysis. Experiments were independently conducted for the assessment of significant differences between the control and experimental groups, and the results were represented by means \pm S.D. Significant differences were determined using Student's *t*-test. Significantly different results were defined as $P < 0.05$.

Conflict of Interest

The authors declare no conflict of interest.

Acknowledgements. We thank Dr. Yu Kang and Dr. Congjian Xu (Fudan University, Shanghai, China) for providing Act-PBase and PB-tk-mRFP plasmids for this work. We thank Dr. Yann-Jang Chen for the technological support of the FISH assay. We thank the facility supported by the Molecular and Genetic Imaging Core/National Research Program for Genomic Medicine at National Yang-Ming University. This study was supported by National Science Council of Taiwan, ROC (NSC 99-2314-B-010-029-MY3; NSC 100-2627-M-010-001; and NSC 101-2623-E-010-002-NU) and a grant from the Ministry of Education, Aim for the Top University Plan, National Yang-Ming University.

1. Steel GG. Cell loss as a factor in the growth rate of human tumours. *Eur J Cancer* 1967; **3**: 381–387.
2. Cooper EH, Bedford AJ, Kenny TE. Cell death in normal and malignant tissues. *Adv Cancer Res* 1975; **21**: 59–120.
3. Serganova I, Mayer-Kukuck P, Huang R, Blasberg R. Molecular imaging: reporter gene imaging. *Handb Exp Pharmacol* 2008; **185/2**: 167–223.
4. Acton PD, Zhou R. Imaging reporter genes for cell tracking with PET and SPECT. *Q J Nucl Med Mol Imaging* 2005; **49**: 349–360.
5. Kircher MF, Gambhir SS, Grimm J. Noninvasive cell-tracking methods. *Nat Rev Clin Oncol* 2011; **8**: 677–688.
6. Diehn M, Clarke MF. Cancer stem cells and radiotherapy: new insights into tumor radioresistance. *J Natl Cancer Inst* 2006; **98**: 1755–1757.
7. Wang HE, Yu HM, Liu RS, Lin M, Gelovani JG, Hwang JJ *et al*. Molecular imaging with ^{123}I -FIAU, ^{18}F -FUDr, ^{18}F -FET, and ^{18}F -FDG for monitoring herpes simplex virus type 1 thymidine kinase and ganciclovir prodrug activation gene therapy of cancer. *J Nucl Med* 2006; **47**: 1161–1171.
8. Haubner R, Avril N, Hantzopoulos PA, Gansbacher B, Schwaiger M. *In vivo* imaging of herpes simplex virus type 1 thymidine kinase gene expression: early kinetics of radiolabelled FIAU. *Eur J Nucl Med* 2000; **27**: 283–291.
9. Love Z, Wang F, Dennis J, Awadallah A, Salem N, Lin Y *et al*. Imaging of mesenchymal stem cell transplant by bioluminescence and PET. *J Nucl Med* 2007; **48**: 2011–2020.
10. Ray P. The pivotal role of multimodality reporter sensors in drug discovery: from cell based assays to real time molecular imaging. *Curr Pharm Biotechnol* 2011; **12**: 539–546.
11. De A, Lewis XZ, Gambhir SS. Noninvasive imaging of lentiviral-mediated reporter gene expression in living mice. *Mol Ther* 2003; **7**: 681–691.
12. Lam AP, Dean DA. Progress and prospects: nuclear import of nonviral vectors. *Gene Ther* 2010; **17**: 439–447.
13. Claeys Bouaert C, Chalmers RM. Gene therapy vectors: the prospects and potentials of the cut-and-paste transposons. *Genetica* 2010; **138**: 473–484.
14. Kim A, Pyykko I. Size matters: versatile use of PiggyBac transposons as a genetic manipulation tool. *Mol Cell Biochem* 2011; **354**: 301–309.
15. Kang Y, Zhang X, Jiang W, Wu C, Chen C, Zheng Y *et al*. Tumor-directed gene therapy in mice using a composite nonviral gene delivery system consisting of the piggyBac transposon and polyethylenimine. *BMC cancer* 2009; **9**: 126.

16. Nakazawa Y, Huye LE, Salsman VS, Leen AM, Ahmed N, Rollins L *et al*. PiggyBac-mediated cancer immunotherapy using EBV-specific cytotoxic T-cells expressing HER2-specific chimeric antigen receptor. *Mol Ther* 2011; **19**: 2133–2143.
17. VandenDriessche T, Ivics Z, Izsvak Z, Chuah MK. Emerging potential of transposons for gene therapy and generation of induced pluripotent stem cells. *Blood* 2009; **114**: 1461–1468.
18. Reya T, Morrison SJ, Clarke MF, Weissman IL. Stem cells, cancer, and cancer stem cells. *Nature* 2001; **414**: 105–111.
19. Zhang M, Rosen JM. Stem cells in the etiology and treatment of cancer. *Curr Opin Genet Dev* 2006; **16**: 60–64.
20. Caruso M, Panis Y, Gagandeep S, Houssin D, Salzmann JL, Klatzmann D. Regression of established macroscopic liver metastases after in situ transduction of a suicide gene. *Proc Natl Acad Sci USA* 1993; **90**: 7024–7028.
21. Visvader JE, Lindeman GJ. Cancer stem cells in solid tumours: accumulating evidence and unresolved questions. *Nat Rev Cancer* 2008; **8**: 755–768.
22. Chiodi I, Belgiovine C, Dona F, Scovassi AI, Mondello C. Drug treatment of cancer cell lines: a way to select for cancer stem cells? *Cancers* 2011; **3**: 1111–1128.
23. Beier D, Hau P, Proescholdt M, Wischhusen J, Oefner PJ, Aigner L *et al*. CD133(+) and CD133(–) glioblastoma-derived cancer stem cells show differential growth characteristics and molecular profiles. *Cancer Res* 2007; **67**: 4010–4015.
24. Broadley KW, Hunn MK, Farrand KJ, Price KM, Grasso C, Miller RJ *et al*. Side population is not necessary or sufficient for a cancer stem cell phenotype in glioblastoma multiforme. *Stem Cells* 2011; **29**: 452–461.
25. Schatton T, Frank MH. The *in vitro* spheroid melanoma cell culture assay: cues on tumor initiation? *J Invest Dermatol* 2010; **130**: 1769–1771.
26. Vlashi E, Kim K, Lagadec C, Donna LD, McDonald JT, Eghbali M *et al*. *In vivo* imaging, tracking, and targeting of cancer stem cells. *J Natl Cancer Inst* 2009; **101**: 350–359.
27. Hermann PC, Bhaskar S, Cioffi M, Heeschen C. Cancer stem cells in solid tumors. *Sem Cancer Biol* 2010; **20**: 77–84.
28. Hart LS, El-Deiry WS. Invincible, but not invisible: imaging approaches toward *in vivo* detection of cancer stem cells. *J Clin Oncol* 2008; **26**: 2901–2910.
29. Borovski T, De Sousa EMF, Vermeulen L, Medema JP. Cancer stem cell niche: the place to be. *Cancer Res* 2011; **71**: 634–639.
30. Tao K, Fang M, Alroy J, Sahagian GG. Imagable 4T1 model for the study of late stage breast cancer. *BMC cancer* 2008; **8**: 228.
31. Frindel E, Malaise EP, Alpen E, Tubiana M. Kinetics of cell proliferation of an experimental tumor. *Cancer Res* 1967; **27**: 1122–1131.
32. Huszthy PC, Giroglou T, Tsinkalovsky O, Euskirchen P, Skaftnesmo KO, Bjerkvig R *et al*. Remission of invasive, cancer stem-like glioblastoma xenografts using lentiviral vector-mediated suicide gene therapy. *PLoS One* 2009; **4**: e6314.
33. Tsai CH, Chiu SJ, Liu CC, Sheu TJ, Hsieh CH, Keng PC *et al*. Regulated expression of cofilin and the consequent regulation of p27(kip1) are essential for G(1) phase progression. *Cell Cycle* 2009; **8**: 2365–2374.
34. Kang Y, Zhang XY, Jiang W, Wu CQ, Chen CM, Gu JR *et al*. The piggyBac transposon is an integrating non-viral gene transfer vector that enhances the efficiency of GDEPT. *Cell Biol Int* 2009; **33**: 509–515.
35. Dierlamm J, Wlodarska I, Michaux L, La Starza R, Zeller W, Mecucci C *et al*. Successful use of the same slide for consecutive fluorescence in situ hybridization experiments. *Genes Chromosomes Cancer* 1996; **16**: 261–264.
36. Yang FY, Wang HE, Lin GL, Teng MC, Lin HH, Wong TT *et al*. Micro-SPECT/CT-based pharmacokinetic analysis of 99mTc-diethylenetriaminepentaacetic acid in rats with blood-brain barrier disruption induced by focused ultrasound. *J Nucl Med* 2011; **52**: 478–484.
37. Loening AM, Gambhir SS. AMIDE: a free software tool for multimodality medical image analysis. *Mol Imaging* 2003; **2**: 131–137.
38. Chew JL, Loh YH, Zhang W, Chen X, Tam WL, Yeap LS *et al*. Reciprocal transcriptional regulation of Pou5f1 and Sox2 via the Oct4/Sox2 complex in embryonic stem cells. *Mol Cell Biol* 2005; **25**: 6031–6046.



Cell Death and Disease is an open-access journal published by Nature Publishing Group. This work is licensed under the Creative Commons Attribution-NonCommercial-No Derivative Works 3.0 Unported License. To view a copy of this license, visit <http://creativecommons.org/licenses/by-nc-nd/3.0/>

Supplementary Information accompanies the paper on Cell Death and Disease website (<http://www.nature.com/cddis>)